Int. J. Dev. Biol. 59: 195-203 (2015)
doi: 10.1387/ijdb.140200md

THE INTERNATIONAL JOURNAL OF DEVELOPMENTAL BIOLOGY
www.intjdevbiol.com

Down-regulation of msrb3 and destruction of normal auditory system development through hair cell apoptosis in zebrafish

XIAOFANG SHEN[1,#], FEI LIU[1,#], YINGZHI WANG[1], HUIJUN WANG[2], JING MA[1], WENJUN XIA[3], JIN ZHANG[1], NAN JIANG[1], SHAOYANG SUN[1], XU WANG[1] and DUAN MA*[,1,2,3]

[1]Key Laboratory of Metabolism and Molecular Medicine, Ministry of Education, Department of Biochemistry and Molecular Biology, Institute of Medical Sciences, School of Basic Medical Sciences, [2]Children's Hospital of Fudan University and [3]Institute of Biomedical Science, School of Basic Medical Sciences, Fudan University, Shanghai, China

ABSTRACT Hearing defects can significantly influence quality of life for those who experience them. At this time, 177 deafness genes have been cloned, including 134 non-syndromic hearing-loss genes. The methionine sulfoxide reductase B3 (Ahmed *et al.,* 2011) gene (also called *DFNB74*) is one such newly discovered hearing-loss gene. Within this gene c.265 T>G and c.55 T>C mutations are associated with autosomal recessive hearing loss. However, the biological role and mechanism underlying how it contributes to deafness is unclear. Thus, to better understand this mutation, we designed splicing morpholinos for the purpose of down-regulating *msrb3* in zebrafish. Morphants exhibited small, tiny, fused, or misplaced otoliths and abnormal numbers of otoliths. Down-regulation of *msrb3* also caused shorter, thinner, and more crowded cilia. Furthermore, L1-8 neuromasts were reduced and disordered in the lateral line system; hair cells in each neuromast underwent apoptosis. Co-injection with human *MSRB3* mRNA partially rescued auditory system defects, but mutant *MSRB3* mRNA could not. Thus, *msrb3* is instrumental for auditory system development in zebrafish and *MSRB3*-related deafness may be caused by promotion of hair cell apoptosis.

KEY WORDS: *deafness, zebrafish, otolith, hair cell, neuromast*

Introduction

Hearing loss is a common but significant birth defect that conveys sensorineural disability (Hilgert *et al.*, 2009) and approximately one of every 1,000 infants has some form of congenital hearing loss (Blanchard *et al.*, 2012). Also, an estimated 28 million Americans, 27.8 million Chinese, and 22.5 million Europeans suffer from hearing defects (Cheng *et al.*, 2011). Sensorineural hearing loss may originate in the organ of Corti within the inner ear (Usami *et al.*, 1998, Kelley, 2007). Sound waves are transferred to the middle ear, vibrating the tympanic membrane, and then ossicles amplify the sound energy and transmit it to the fluid-filled cochlea. Eventually, these movements are converted into fluctuations in the basilar membrane and then into changes in the relative positions of stereocilia and tectorial membranes, stimulating hair cells. Then, hair cells convert this mechanical energy into electrical signals. The organ of Corti is composed of hair cells, supporting cells, and stereocilia, and a slight damage to this organ can cause serious hearing impairment (Borck *et al.*, 2011, Dror and Avraham, 2010, Gillespie and Muller, 2009, Frolenkov *et al.*, 2004). Hair cells, supporting cells, stereocilia, and otoliths in zebrafish have functions similar to their human counterparts. Furthermore, research suggests that the necessary genes for normal hearing account for nearly 1% of all human genes (Friedman and Griffith, 2003). At this time, 177 deafness genes have been cloned (http://hereditaryhearingloss.org/main.aspx?c=.HHH&n=86307), which is a substantial advance in deafness research, but the pathogenic mechanisms underlying how these deafness genes (such as *MSRB3*) cause hearing loss are not understood.

Researchers have identified methionine sulfoxide reductase B3 (*MSRB3*) as a deafness gene via sequencing the genes of affected

Abbreviations used in this paper: MSRB3, methionine sulfoxide reductase B3.

***Address correspondence to:** Duan Ma. Key Laboratory of Molecular Medicine, Ministry of Education, Shanghai Medical College, Fudan University, Shanghai 200032, China. Tel: 021-5423-7441. E-mail: duanma@fudan.edu.cn

#Note: The indicated authors contributed equally to this work.

Accepted: 28 May 2015.

ISSN: Online 1696-3547, Print 0214-6282

individuals. This gene can repair proteins damaged by oxidative stress by catalyzing methionine sulfoxides, reducing them to their corresponding methionines (Weissbach *et al.*, 2002). *MSRB3* has four transcripts encoding two isoforms (MSRB3A and MSRB3B). *MSRB3A* is predicted to exist in the endoplasmic reticulum, and MSRB3B may be within the mitochondria. Two homozygous mutations, c.265T>G and c.55T>C, were reported to be deafness mutations of *MSRB3* (Ahmed *et al.,* 2011*).* The c. 265 T > G mutation can lead to loss of activity of MSRB3A, and the c. 55 T > C mutation is a truncating mutation. Thus, these data suggest that functional *MSRB3* is critical to human hearing. In an attempt to better understand the pathogenesis of *DFNB74* deafness caused by *MSRB3* deficiency, Kwon's group generated *Msrb3* knockout mice using homologous recombination and reported that *Msrb3* deficiency caused progressive degeneration of stereocilia, followed by hair cell apoptosis and that this caused profound deafness in *Msrb3*$^{-/-}$ animals (Kwon *et al.*, 2014).

Zebrafish do not have an outer or middle ear, but instead have a typical vertebrate inner ear, which has been previously described (Whitfield, 2002, Waterman and Bell, 1984, Haddon and Lewis, 1996, Bang *et al.*, 2001, Bever and Fekete, 2002). Also, zebrafish have a lateral line system of neuromasts containing hair cells whose stereocilia are directly exposed to the water, sensing movement along the head and body surface. Unlike inner ear hair cells, neuromasts are present on the animal surface, making them highly accessible and easy to study (Ma *et al.*, 2008, Nagiel *et al.*, 2008, He *et al.*, 2013). Finally, *msrb3* homology between *Homo sapiens* and *D. rerio* is as high as 84.87%, which confirms that zebrafish are a suitable animal model for studying vertebrate ear development and function (Wu *et al.*, 2010, Whitfield, 2002). Here, we describe *Msrb3* knockout zebrafish, which we used to investigate how *DFNB74* contributes to deafness caused by the loss of MSRB3.

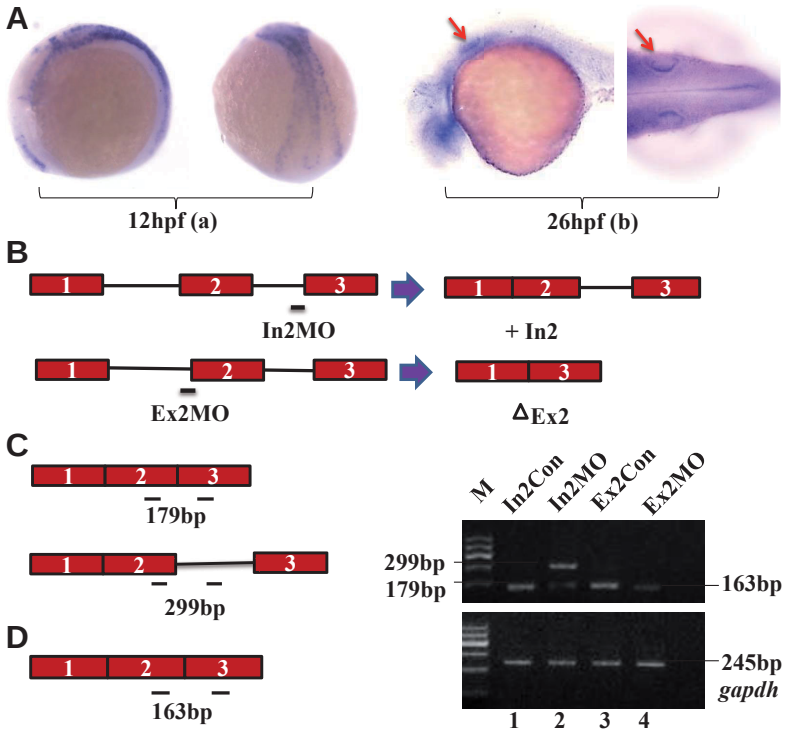

Fig. 1. Efficiency of *msrb3* morpholinos. (A) *WISH at 12 hpf showed that* msrb3 *was widely expressed in embryos (a). At 26 hpf* msrb3 *was highly expressed in the inner ear of embryos (b).* **(B)** *Morpholino antisense oligonucleotides.* **(C)** *Primers designed to measure efficiency of In2MO (179 bp and 299 bp products).* **(D)** *Primers designed to measure efficiency of Ex2MO (less 163 bp product).* **(E)** *Morpholino efficiency: two* msrb3 *morpholinos could interfere with normal mRNA splicing (compare lane 1 to lane 2 and lane 3 to lane 4).*

Results

Two kinds of morpholinos can knock down the expression of msrb3

Whole-mount *in situ* hybridization (WISH) at 12 and 26 hours post fertilization (hpf) revealed that *msrb3* was widely expressed in embryos, especially in the inner ear (Fig. 1A). To understand how msrb3 works, two splice morpholinos were designed to down-regulate normal *msrb3* expression in zebrafish. Binding of these two morpholinos at their respective binding sites caused retention of intron2 and loss of exon2 (Fig. 1B). After microinjection, the efficiency of In2MO and Ex2MO was measured with RT-PCR. Primers designed to measure In2MO efficiency were expected to produce a 179 bp product in control embryos (In2Con), and morphants were expected to produce a 299 bp product (In2MO) (Fig. 1C). Primers designed to confirm the efficiency of Ex2MO should yield morphants (Ex2MO) without the 163 bp product found in control embryos (Ex2Con) (Fig. 1D). RT-PCR showed that the expression of *msrb3* was largely down-regulated (Fig. 1E).

Decreased msrb3 *caused otic developmental defects*

To learn whether *msrb3* is essential to zebrafish otic development, morphant phenotypes were observed and compared to controls. First, morphology of controls (Fig. 2A a,c) and *msrb3* morphants (Fig. 2A b,d) were observed at 60 hpf, and *msrb3* morphants had otolith abnormalities. Otic vesicles visualized with DIC microscopy revealed that by 60 hpf, two otoliths appeared in control embryos (Fig. 2A e, k) and the otolith closer to the eyes was smaller. However, *msrb3* morphants exhibited tiny (Fig. 2A f,l), fused (Fig.2A h,n), misplaced (Fig. 2A l,o), or small (Fig. 2A j,p) otoliths, abnormal otolith numbers (Fig. 2A g,m), and malformed semicircular canals (Fig. 2A f–g, l–p). A quantitative analysis of otolith defects of both morphants was performed at 60 hpf. Fish with the defect are depicted in Fig. 2 B,C. Each experiment was performed in triplicate and otolith abnormalities in controls and *msrb3* morphants were statistically significantly different (Fig. 2 D,E).

Msrb3 *is essential for the development of cilia in inner ear and lateral line neuromasts*

Inner ear sterecilia of 5 dpf zebrafish were marked with FITC-labelled phalloidin and observed under confocal microscopy. *Msrb3* morphants (Fig. 3 B,D) had semicircular canal defects not present in controls (Fig. 3 A,C). Sterecilia of *msrb3* morphants (Fig. 3 B,D) were shorter and more crowded than controls. Kinocilia in lateral line neuromasts were observed under SEM and these were shorter in morphants (Fig. 3 E–H). Statistical analysis of inner ear sterecilia (Fig.3I) and neuromasts kinocilia(Fig.3J) in mismatch controls and msrb3 morphants indicated statistical significance.

Decreased msrb3 *caused disordered neuromasts and fewer hair cells*

Zebrafish have a special lateral line system composed of neuromasts containing hair and supporting cells (Ghysen, 2003). We labeled hair cells with a transgenic fish: Tg (Brn3c:mGFP) S356T transgenic zebrafish expressing GFP in hair cells under control of the POU4F3 promoter that is targeted to the plasma membrane with a GFP-43 membrane targeting sequence. Hair cells in neuromasts were visualized by allowing embryonic zebrafish to swim in FM-1-43FX (red) dye which binds to nerve cell membranes via a mechanotransduction channel (Gleason *et al.*, 2009). Then larvae were fixed in 4% paraformaldehyde and nuclei were labeled with DAPI (blue) to visualize neuromasts and hair cells. Down-regulation of *msrb3* produced fewer and disordered lateral line neuromasts (Fig. 4 A,B) and fewer neuromast hair cells (Fig. 4 D,E). Statistical analysis of L1-8 neuromasts (Fig. 4C) and hair cells per neuromast (Fig. 4F) in mismatch controls and *msrb3* morphants were significantly different.

Msrb3 *deficiency leads to apoptotic hair cell death in neuromasts*

A TUNEL assay was performed with a TMR-RED *in situ* cell death detection kit. Results showed significantly more apoptotic hair cells in neuromasts of 3 dpf morphants than in those of controls (Fig. 5 A,B). Statistical analysis of apoptotic hair cells per neuromast in mismatch controls and msrb3 morphants indicated statistical significance (Fig. 5C).

Technologies used to study gene functions by sequence-specific knockdown can elicit undesirable off-target effects. About 15–20% of morpholinos used in zebrafish have off-targeted effects (Ekker and Larson, 2001). Although not all underlying causes of off-target effects were clear, most of these were mediated via *p53* activation which is well described (Robu *et al.*, 2007, Gerety and Wilkinson, 2011). To rule out the possibility of whole-body apoptosis mediated by *p53*,

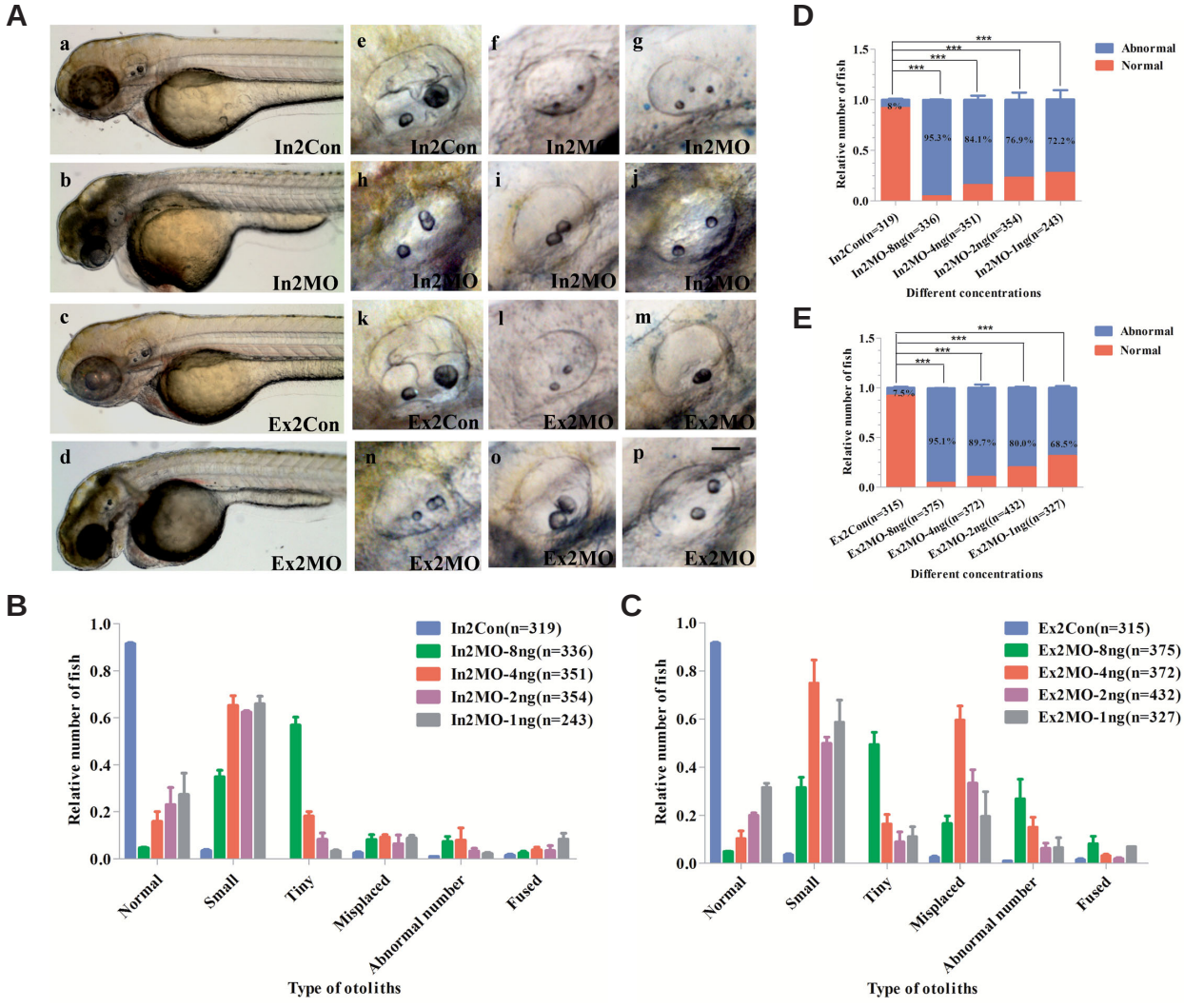

Fig. 2. Otic developmental defects in *Msrb3* morphants. (A) *Overall morphology of mismatched controls (In2Con, a; Ex2Con, c) and* msrb3 *morphants (In2MO, b; Ex2MO, d) at 60 hpf indicated otolith abnormalities. Otic vesicles were visualized at 60 hpf using DIC microscopy. Scale bars: 50 μm. Unlike mismatch control (e; k),* msrb3 *morphants had tiny otoliths (f, l), abnormal otolith numbers (g, m), fused otoliths (h, n), misplaced otoliths (i, o), small otoliths (j, p), shrunken inner ears, and malformed semicircular canals (f–g, l–p).* **(B,C)** *Quantitative analysis of otolith defects of In2MO and Ex2MO at different concentrations at 60 hpf. Relative number of fish with otic developmental defects.* **(D,E)** *Statistical analysis of otolith abnormalities in controls and* msrb3 *morphants. Error bars are s.d. ***P<0.0001.*

larvae were injected with *msrb3* morpholinos (In2MO, Ex2MO) or co-injected with *msrb3* morpholinos and p53MO. Acridine orange staining was used to detect whole apoptosis signals of larvae at 24 hpf. There were no obvious differences in apoptotic signals between whole *msrb3* morphants and p53MO co-injected larvae (Fig. 5 D,E). Thus, the morpholino off-target effect was ruled out.

Human MSRB3A *mRNA can rescue otic defects in msrb3 morphants*

Down-regulation of *msrb3* caused otic developmental defects in zebrafish. This gene shares 68.28% homology with human *msrb3* (Fig. 6A). Therefore, human *MSRB3A* and *MSRB3A*-265T>G were obtained (Fig. 6B) and transcribed into mRNA and human *MSRB3A* mRNA or *MSRB3A-265T>G* mRNA was injected into zebrafish embryos with morpholinos to determine whether *MSRB3A* mRNA from humans could rescue defects caused by reduced *msrb3* expression. Results show that human *MSRB3A* mRNA but not the mutant *MSRB3A* mRNA could significantly rescue otic defects of zebrafish morphants (Fig. 6 C,D). Finally, controls and different *msrb3* morphants were significantly different (Fig. 6 E,F).

Msrb3 morphants at 6 dpf had hearing loss

The inner ear is critical for crucial roles in zebrafish hearing and balance. After inducing inner ear defects in *msrb3* morphants, swimming and hearing were investigated and we observed that larvae injected with control morpholinos usually swam or rested with their backs facing up and swam at a consistent depth. However, *msrb3* morphants remained stationary and rested in abnormal positions, swimming up and down or in circles. The abnormal swimming behavior of *msrb3* morphants indicated a defective balance system.

To confirm hearing impairment, the C-shaped startle response was also tested using near-field pure tone stimulation with sound intensity (500 Hz, 80 dB). The C-startle response of morphants took longer to manifest than control larvae, especially those with very small otoliths. Some morphants had no response to voice stimulation. After co-injection with human *MSRB3A* mRNA (*hM3A*), about half of the morphants regained some hearing (Fig. 7 B,D). Morphant swimming postures tended to normalize, and audio stimulus sensitivity was greatly increased (Fig. 7 A,C). These findings support the idea that *msrb3* is key to zebrafish hearing.

Discussion

Hair cells, supporting cells, and cilia are so important that even slight damage can cause serious hearing impairment in both humans and zebrafish (Dror and Avraham, 2010, Gillespie and Muller, 2009, Frolenkov *et al.*, 2004, Borck *et al.*, 2011). Morphogenesis of zebrafish otic vesicles has been described in detail (Kimmel *et al.*, 1995, Haddon and Lewis, 1996) and in this depiction, the zebrafish embryonic inner ear appears as a solid otic placode near the hindbrain by 13.5 hpf. Then the placode hollows out into the otic vesicle at 18.5 hpf. Precursor dispersal particles in otic vesicles are attracted by vortices caused by stereocilia

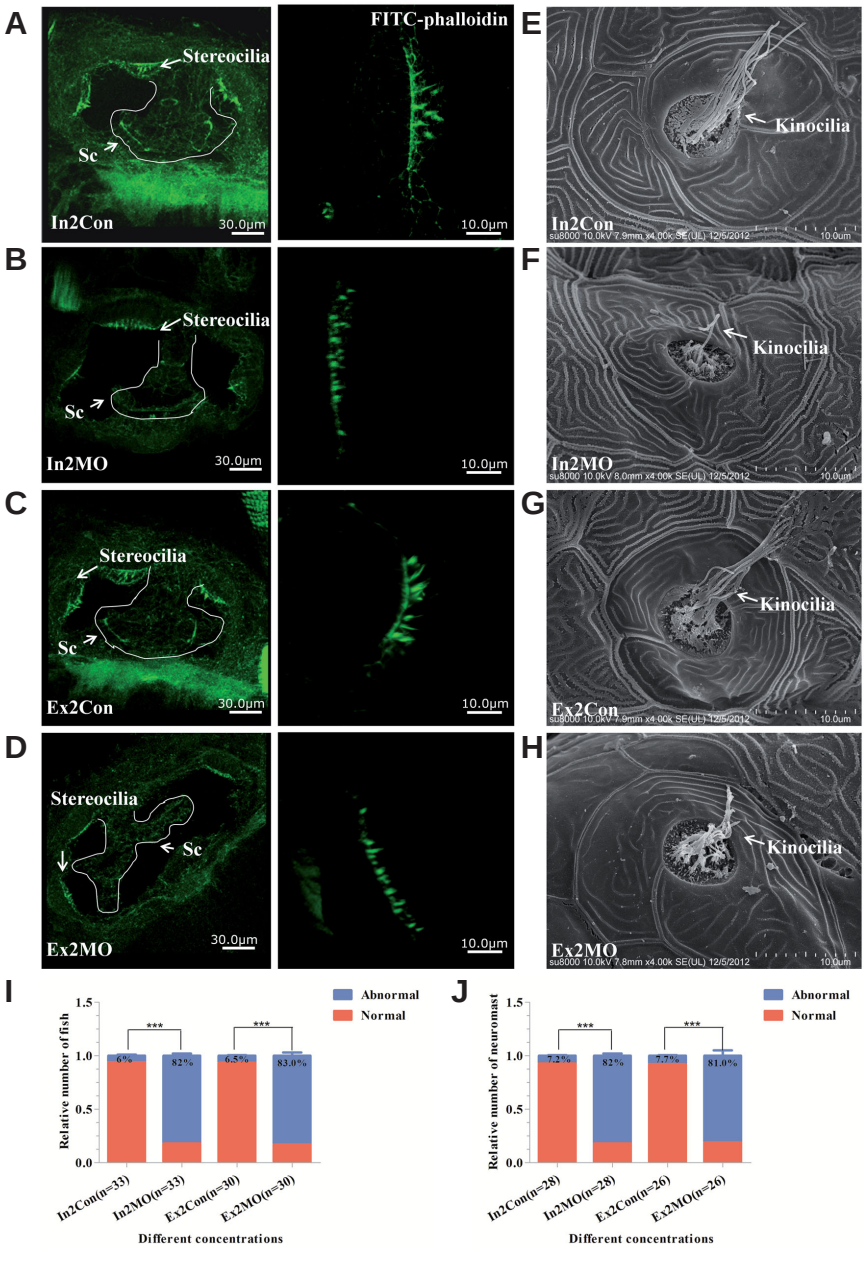

Fig. 3. Cilia damage in *Msrb3* morphants. (A–D) *Stereocilia in zebrafish inner ear marked with FITC-labeled phalloidin (confocal microscopy). Stereocilia in* msrb3 *morphants (In2MO, Ex2MO) were shorter and thinner than those of mismatch controls (In2Con, Ex2Con). In addition,* msrb3 *morphants had malformed semicircular canals. Scale bars: 30 μm.* **(E–H)** *Kinocilia in lateral line neuromasts of morphants were damaged (not see in controls). Scale bars: 10 μm.* **(I)** *Statistical analysis of inner ear stereocilia in controls and* msrb3 *morphants, "n" represents fish number. Error bars are s.d. ***P<0.0001.* **(J)** *Statistical analysis of neuromast kinocilia in controls and* msrb3 *morphants, "n" represents neuromasts number. Error bars are s.d. ***P<0.0001.*

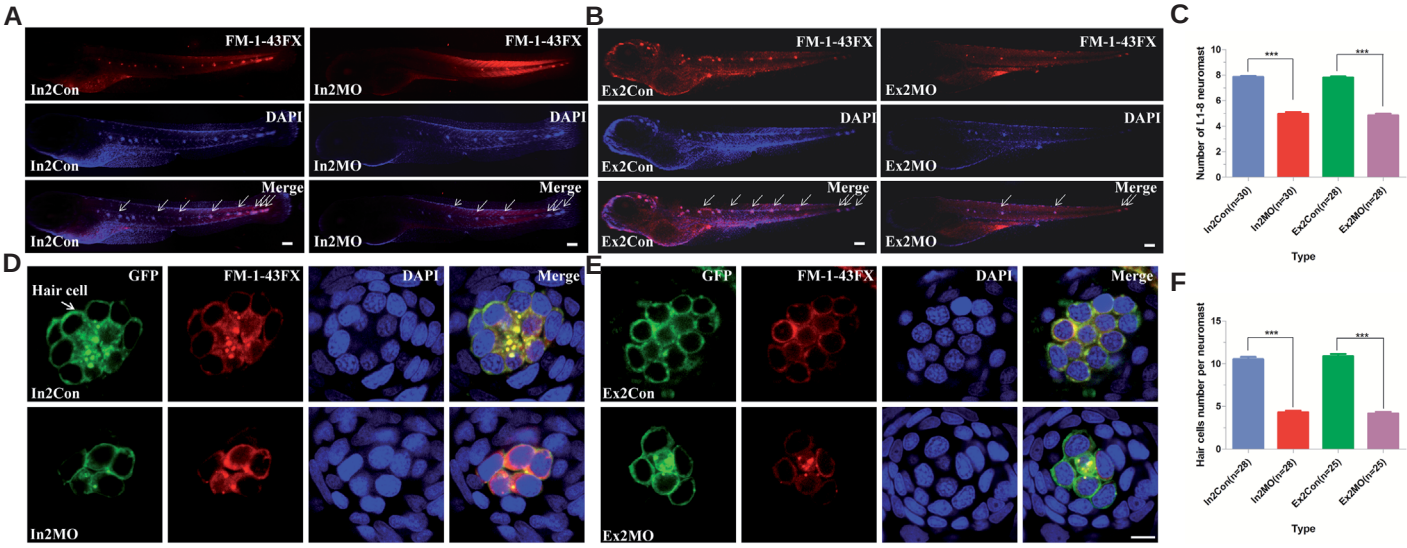

Fig. 4. Down-regulation of *msrb3*. L1-8 neuromasts were decreased and disordered and hair cells were reduced. (A,B; D,E) *Hair cells in lateral line neuromasts stained with FM-1-43FX.* **(A,B)** *In2MO and Ex2MO morphants had fewer and more disordered primary neuromasts than controls. Scale bars: 150 μm.* **(D,E)** Msrb3 *morphants had fewer hair cells per neuromast than controls. Scale bars: 5 μm.* **(C)** *Statistical analysis of the L1-8 neuromasts in mismatch controls and msrb3 morphants, "n" represents fish number.* **(F)** *Statistical analysis of hair cells per neuromast in mismatch controls and msrb3 morphants, "n" represents neuromasts number. Error bars are s.d. ***P<0.0001.*

motility and together facilitate the otolith formation (Nayak *et al.*, 2007, Colantonio *et al.*, 2009). Generally, otoliths appeared at 22 hpf, and became prominent by the prim-6 stage (25 hpf) in the otic vesicle, enlarging along as stereocilia acquired regular motility. The primordia of the semicircular canals formed at 60 hpf, separating vesicles into otolith-containing chambers. By then, otolith morphology was stable. Thus, 60 hpf was selected as the end of otolith observation and statistical analysis.

An autosomal recessive non-syndromic sensorineural hearing loss has been reported to be related to a homozygous single nucleotide conversion (265T>G) of *MSRB3* in the six DFNB74 families (Ahmed *et al.*, 2011). There are seven transcripts of *msrb3* in zebrafish, one of which has no protein product (http://www.ensembl.org). Two splicing morpholinos were designed to down-regulate the other six *msrb3* transcripts simultaneously. In our hands, down-regulation of *msrb3* in zebrafish contributed to progressive degeneration of stereocilia, followed by apoptotic hair cells, resulting in profound deafness in *msrb3* morphants. These phenotypes are highly consistent with data from *Msrb3*$^{-/-}$ mice. Thus, *msrb3* plays an important role in hair cell integrity

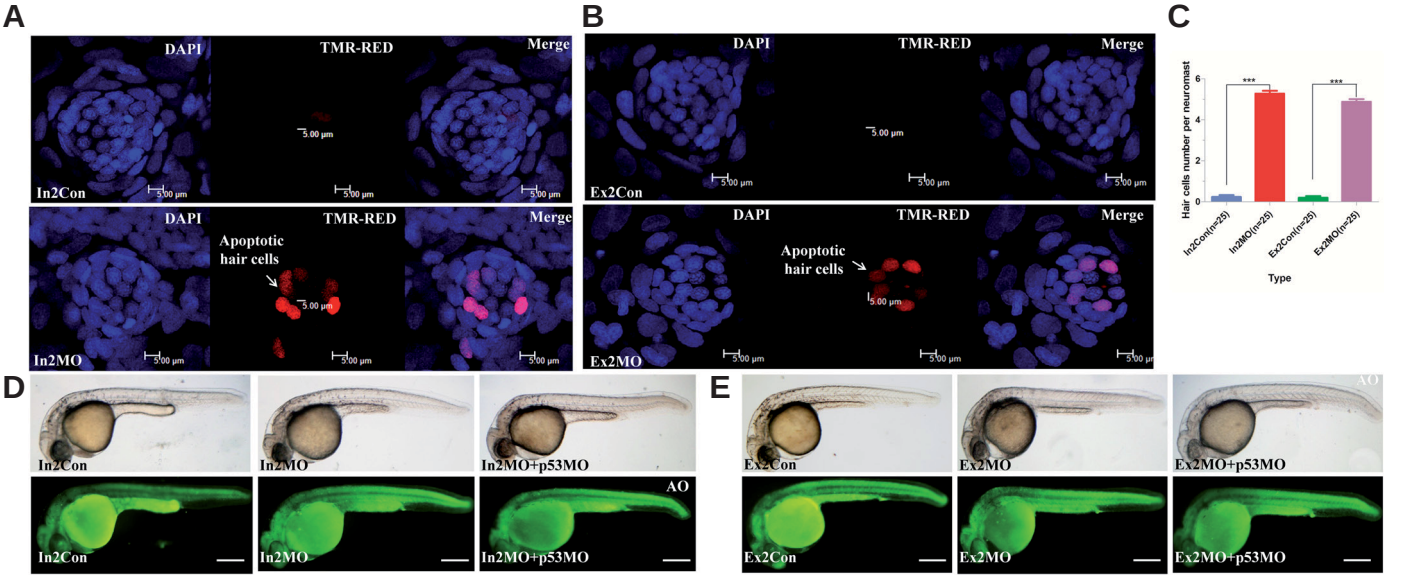

Fig. 5. *Msrb3* morphant apoptotic hair cells. (A,B) *TUNEL assay data. In 3 dpf larvae,* msrb3 *morphants had more hair cell apoptosis than mismatch controls. Scale bars, 5 μm.* **(C)** *Statistical analysis of apoptotic hair cells per neuromast in controls and msrb3 morphants, "n" represents neuromasts number. Error bars are s.d. ***P<0.0001.* **(D,E)** *Zebrafish embryos injected with* msrb3 *morpholinos (In2MO, Ex2MO) or co-injected with* msrb3 *morpholinos and p53MO—AO staining to detect whole larval apoptosis signal at 24 hpf. There was no difference between* msrb3 *morphants and p53MO co-injected larvae. The* p53 *off-target effect was ruled out. Scale bars, 200 μm.*

cells, possibly accounting for the pathogenesis behind hearing loss caused by an *MSRB3* deficiency.

MSRB3 is widely expressed in mice and zebrafish. Previous reports indicate that no other disease is caused by this deafness-related mutation in humans (Ahmed *et al.*, 2011). However, some phenotypes not related to hearing were observed in zebrafish morphants. These were characterized by disorganized somites, hydrocephaly, and pericardial effusion. It also is necessary to confirm whether other organs are affected at later stages of development.

The methionine sulfoxide reductase family (Msr) contains both methionine-*S*- sulfoxide reductase (MsrA) and methionine-*R*-sulfoxide reductase (MsrB). These compounds play important roles in reducing methionine sulfoxide to methionine (Kim and Gladyshev, 2004, Weissbach *et al.*, 2005) which can repair proteins damaged by oxidative stress as well as regulate the lifespans of several organisms (Lee *et al.*, 2009). Ahmed reported that *MSRB3* isoforms targeted to mitochondria were essential to hearing and this group concluded that loss of function of *msrb3* led to progressive cilia damage, followed by apoptosis of hair cells, which caused profound deafness in *msrb3* morphants. Furthermore, these morphants similar to phenotypes observed in

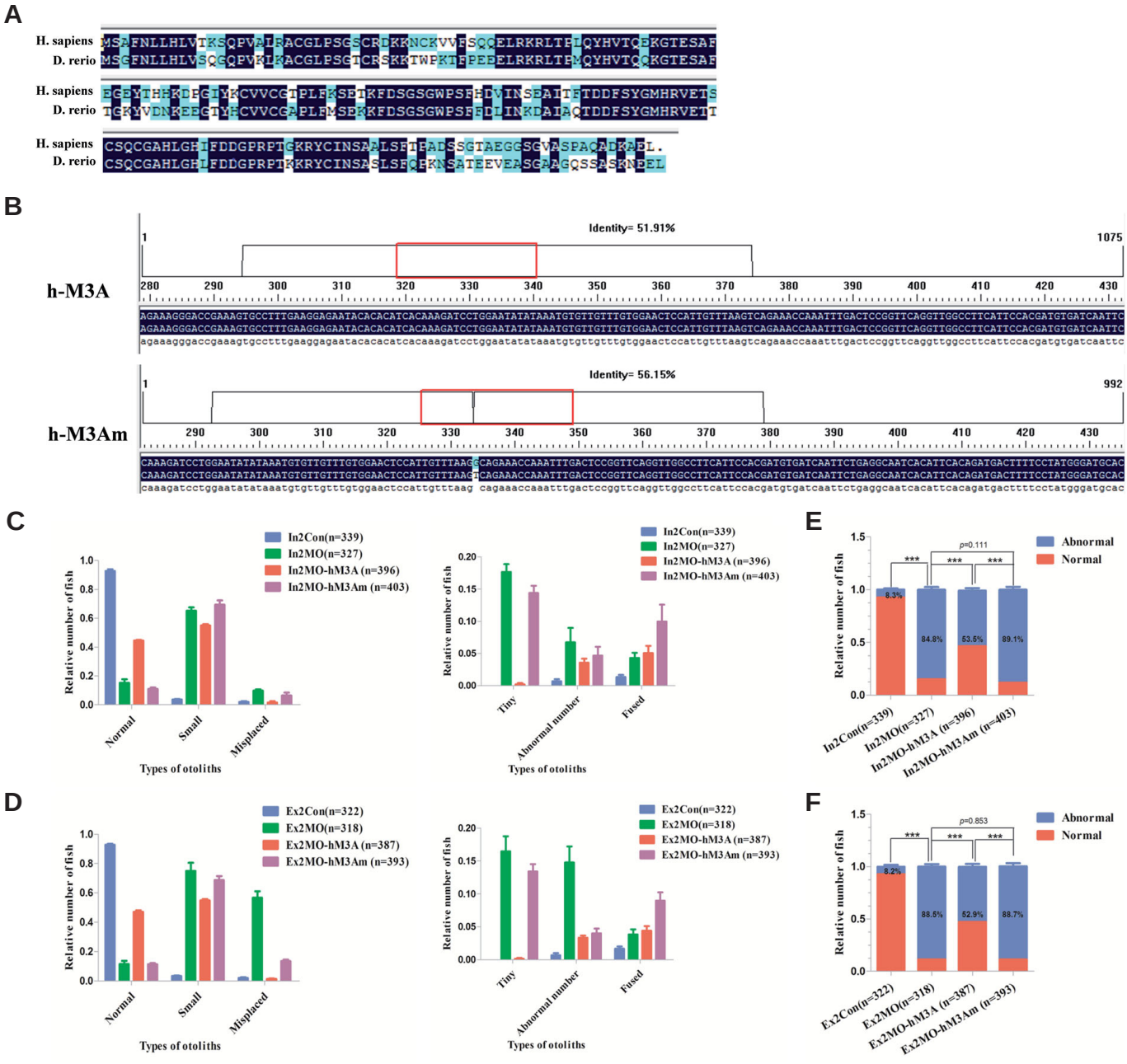

Fig. 6. *MSRB3* comparisons. (A) *Amino acid sequence comparison of* MSRB3A *between* Homo sapiens *and* Danio rerio *(68.28% homology).* **(B)** *Human* MSRB3A *and* MSRB3A *mutants were obtained and transcribed into mRNA.* **(C,D)** *Overexpression of human* MSRB3A *mRNA rescued otic defects in morphants, but human* MSRB3A *mutant did not. Error bars are s.d.* **(E,F)** *Statistical analysis of otolith abnormality in different types of larvae. Human* MSRB3A *mRNA but not mutant* MSRB3A *mRNA rescued otic developmental defects. Error bars are s.d.* ***P<0.0001.

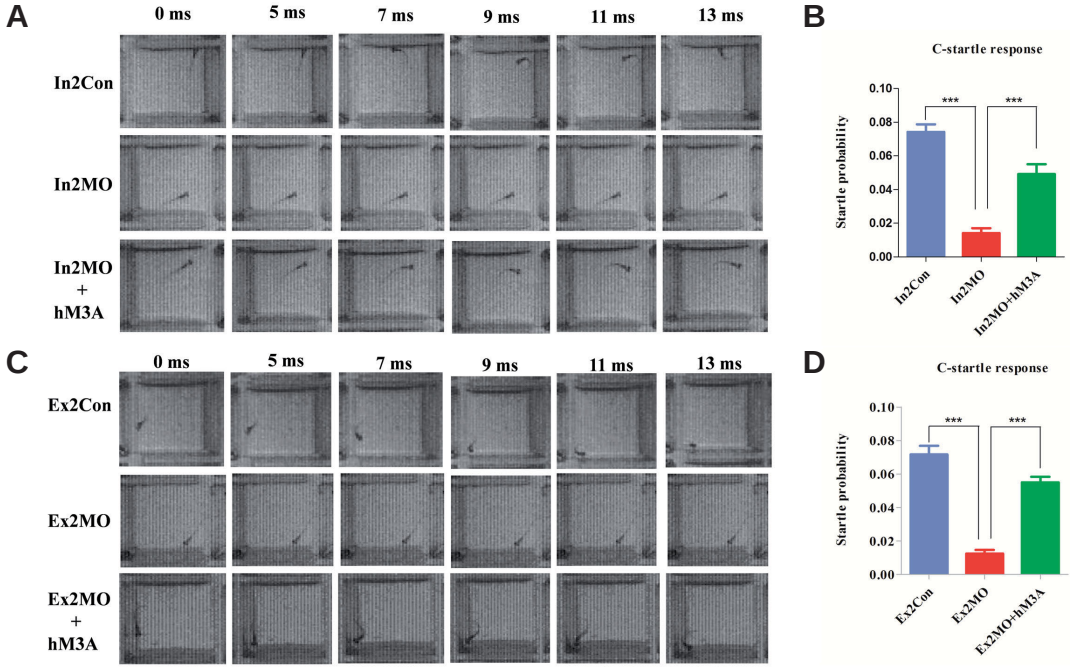

Fig. 7. *Msrb3* morphants are profoundly deaf. (A,C) *Examples of C-shaped startle responses of different larval types after sound stimuli (500 Hz; 10 ms). The escape response of control larvae was initiated 5–13 ms after the sound stimulation. Abnormal swimming behavior of* msrb3 *morphants indicated a defective balance system. Some morphants had no response to voice stimulation. After co-injection with human* MSRB3A *mRNA (hM3A), In2MO and Ex2MO zebrafish regained some hearing.* **(B,D)** *Average C-startle response probability. For each group, 30 larvae were tested.* *** $P<0.0001$.

the *DFNB74* patients (Ahmed *et al.*, 2011). In summary, we have offered a foundation for studying the pathogenesis of *DFNB74* deafness, and we have established that the *msrb3* morphant is a suitable animal model for further research into the mechanisms underlying human DFNB74 hearing loss.

Materials and Methods

Zebrafish lines

The zebrafish AB line was used and these were raised according to the standard protocol described in *The Zebrafish Book.* Transgenic pou3f4-GFP zebrafish embryos were provided by Dr. Huawei Li. Embryos were kept at 28.5 °C and 0.003% 1-phenyl-2-thiourea (PTU, Sigma) was used to suppress pigmentation (Karlsson *et al.*, 2001). Developmental stages were judged by hpf and number of somites (S). Experimental procedures and animal use and care protocols were approved by the Fudan University Animal Ethics Committee.

Morpholino antisense oligonucleotides and microinjection

Two morpholino antisense oligonucleotides were designed to prevent correct splicing of *msrb3* in zebrafish. One morpholino (+intron2MO, In2MO) targeted the splice junction between intron2 and exon3, causing intron2 to be retained. The other one (Δexon2MO, Ex2MO) targeted the splice junction between intron1 and exon2, causing exon2 to be removed. Mismatch controls allowed researchers to interpret morpholino experiments correctly and completely (Eisen and Smith, 2008). In2MO: 5′-TGTCAAACCGTGTGACACACCTCTC-3′; In2Con: 5′-TGTgAAAgCcT GTcACAgACCTCTC-3′; Ex2MO: 5′-CACGTTCCTAATGGAAATACAAGCA-3′; Ex2Con: 5′-CACcTTgCTAATcGAAATAgAAcCA-3′. All sequences were obtained from Gene Tools Website (http://www.gene-tools.com/Oligo_Design). After synthesis, morpholinos were diluted with RNase-free water (Takara).

Morpholinos were injected into embryos at the one-cell stage (Xu, 1999). with either 8, 4, 2, or 1 of one type splicing morpholino (In2MO, Ex2MO) or with 4 ng mismatch control morpholinos (In2Con, Ex2Con).

Human *MSRB3A and MSRB3A-265T>G* were amplified through reverse transcription PCR (RT-PCR) and verified by sequencing. DNA generated by PCR can be transcribed directly from the PCR provided it contains a T7 RNA polymerase promoter upstream of the sequence to be transcribed. Then *MSRB3A* and *MSRB3A-265T>G* mRNA were synthesized *in vitro* according to the instructions provided with the mMESSAGE mMACHINE® T7 Ultra Kit (Ambion).

RT-PCR

Reverse transcription PCR was performed as described previously (Zhao *et al.*, 2010). Primer pairs used in reverse transcription PCR to detect the knockdown efficiency of In2MO are 5′-GACATGGCCTAAAACGTTCC-3′ (forward in exon 2) and 5′-AAGAGGTGCAC CGCAAAC-3′ (reverse in exon3) or 5′-GCTCATTTTGG TGGTACTTCG-3′ (reverse in intron2). The two primer pairs yielded 179 bp (normal splicing) or 299 bp (intron 2 retained). If the mRNA of *msrb3* was correctly spliced, the primer combination produces a 179 bp product. If intron2 is retained, a 299 bp results. Primers used to assess the efficiency of Ex2MO down-regulation were 5′-CGTGCCGAAGTAAGAAGACA-3′ (forward in exon 2) and 5′-AAGAGGTGCA CCGCAA AC-3′ (reverse in exon 3) and these primers produced a 163 bp product. If exon 2 had been removed, less of this product would be evident.

Whole-mount in situ hybridization (WISH)

Msrb3 complementary DNA of zebrafish was subcloned into the vector pGEM®-T by PCR amplification with 5′-CGCTGTTTCTGTT CACCC-3′ (forward) and 5′-TCCGACCAATGTTGC TAA-3′ (reverse). pGEM-*msrb3* was linearized using SalI and the antisense digoxigenin-UTP-labeled full-length riboprobe was transcribed using T7 RNA polymerase (Promega). Zebrafish embryos were collected at different stages of development, washed three times with PBST in DEPC, and fixed in 0.5 ml 4% paraformaldehyde for 5 min at room temperature. Then paraformaldehyde was removed and samples were fixed in another 0.5 ml paraformaldehyde for 12–16 h at 4 °C before WISH which was performed primarily as described previously (Chen and Fishman, 1996, Tian *et al.*, 2009, Le Guellec *et al.*, 2004). Anti-digoxigenin antibody (Roche) was used to detect *msrb3* mRNA signals.

FM-1-43FX and phalloidin staining

Hair cells in lateral line neuromasts were labeled by immersing 5 dpf larvae in a solution of FM1-43FX (Invitrogen) in breeding water for 1–2 min at room temperature, and then the water was changed several times until clear. Zebrafish were immobilized in 1% low melting point agarose gel and labeled hair cells were imaged under a confocal microscope. Cilia in the inner ears of 5 dpf zebrafish were marked with 2.5 mg/ml fluorescein

isothiocyanate (FITC)-labeled phalloidin (Sigma) in PBS for 2 h in the dark after immersion in 4% paraformaldehyde and then incubated overnight at 4 °C in 2% Triton X-100 (Sigma) in PBS. Then embryos were washed several times in PBS over the course of 2 h and viewed with a confocal microscope (Leger and Brand, 2002).

Scanning electron microscopy (SEM)

All SEM images were taken of larvae at 5 dpf. This stage is early enough to observe many developing hair bundles, but late enough to adequately preserve larvae. For our sequential analysis individual larvae were anesthetized with 0.03% MESAB and pinned onto a Sylgard-filled chamber. After imaging, the cupula surrounding neuromasts was removed by incubating larvae in a high dose of MESAB (0.12%) for 25s. Specimens were then fixed in 2.5% glutaraldehyde, 2 mM $CaCl_2$ in 0.1 M cacodylate buffer for 2 hrs at room temperature. Samples were washed and post-fixed in 80 mM cacodylate buffer and 4 mM $CaCl_2$ for 10 min on ice. Embryos were washed five times with water and then dehydrated in steps from 50% to 100% ethanol at room temperature. Larvae were then critical point dried and mounted on carbon covered aluminum stubs. The head and tail tip of each larvae were painted with silver to minimize charging. Lastly samples were sputter coated with gold-palladium. A FEI Sirion XL30 scanning electron microscope was used to acquire images.

Apoptosis detection

TUNEL assay was detected with TMR-RED *in situ* cell death detection kit (Roche). Then, 3 dpf embryos were dechorionated and fixed in 4% PFA paraformaldehyde overnight at 4 °C, immersed in methanol for 1 h at room temperature, and washed three times with PBST. Samples were incubated in acetone at -20 °C for 10 min, permeabilized with 0.1% sodium citrate and 0.1% TritonX-100 for 15 min at room temperature, and washed twice in PBST buffer. Samples were then incubated with the reaction mixture (5 μl of enzyme solution + 45 μl label solution) for 1 h in the dark at 37 °C. The reaction was stopped by washing three times with PBST. The fluorescent signal was visualized and imaged using a Zeiss LSM510 microscope.

Acridine orange staining

Acridine orange (AO) staining was used to detect apoptotic signals in whole zebrafish larvae to rule out p53 off-target effects (Abrams *et al.*, 1993). Larvae at 24 hpf were immersed in 2 μg/ml AO in the dark in breeding water for 1 h at room temperature. Then larvae were washed three times with breeding water for 10 min each. Images were obtained with DIC microscopy.

Startle response tests

The C-shaped startle response using near-field pure tone stimulation with sound intensity was used to test larval hearing (Bang *et al.*, 2002). This experiment was tested in 96-well plastic plates, and recorded with a high-speed camera (Redlake, MotionScope M3, 1,000 fps) under infrared light illumination. Pure tone stimulations (10 ms, 500 Hz) at two different intensities were given through a plastic board mounted on a voice box (HiVi, D1080MKII). Each larva was tested 13–15 times and the relative number of C-startle responses was calculated for each larva. The probability of the C-startle response for a larval group was the average percentage of C-startle reflexes (Han *et al.*, 2011).

Statistical analysis

Statistical analysis was performed using two-way ANOVA with multiple comparisons. Significance was set at $P<0.05$ and extreme significance was set at $P<0.001$.

Acknowledgments and funding

This study was supported by the National Basic Research Program of China (2011CB504500), Foundation of Ministry of Health (201202005), Shanghai Scientific and Technology Projects (2013ZYJB0015 and 14DJ1400103).

References

ABRAMS, J. M., WHITE, K., FESSLER, L. I. and STELLER, H. (1993). Programmed cell death during *Drosophila* embryogenesis. *Development* 117: 29-43.

AHMED, Z. M., YOUSAF, R., LEE, B. C., KHAN, S. N., LEE, S., LEE, K., HUSNAIN, T., REHMAN, A. U., BONNEUX, S., ANSAR, M., AHMAD, W., LEAL, S. M., GLADYSHEV, V. N., BELYANTSEVA, I. A., VAN CAMP, G., RIAZUDDIN, S. and FRIEDMAN, T. B. (2011). Functional null mutations of MSRB3 encoding methionine sulfoxide reductase are associated with human deafness DFNB74. *Am J Hum Genet* 88: 19-29.

BANG, P. I., SEWELL, W. F. and MALICKI, J. J. (2001). Morphology and cell type heterogeneities of the inner ear epithelia in adult and juvenile zebrafish (Danio rerio). *J Comp Neurol* 438: 173-190.

BANG, P. I., YELICK, P. C., MALICKI, J. J. and SEWELL, W. F. (2002). High-throughput behavioral screening method for detecting auditory response defects in zebrafish. *J Neurosci Methods* 118: 177-187.

BEVER, M. M. and FEKETE, D. M. (2002). Atlas of the developing inner ear in zebrafish. *Dev Dyn* 223: 536-543.

BLANCHARD, M., THIERRY, B., MARLIN, S. and DENOYELLE, F. (2012). [Genetic aspects of congenital sensorineural hearing loss]. *Arch Pediatr* 19: 886-889.

BORCK, G., UR REHMAN, A., LEE, K., POGODA, H. M., KAKAR, N., VON AMELN, S., GRILLET, N., HILDEBRAND, M. S., AHMED, Z. M., NURNBERG, G., ANSAR, M., BASIT, S., JAVED, Q., MORELL, R. J., NASREEN, N., SHEARER, A. E., AHMAD, A., KAHRIZI, K., SHAIKH, R. S., ALI, R. A., KHAN, S. N., GOEBEL, I., MEYER, N. C., KIMBERLING, W. J., WEBSTER, J. A., STEPHAN, D. A., SCHILLER, M. R., BAHLO, M., NAJMABADI, H., GILLESPIE, P. G., NURNBERG, P., WOLLNIK, B., RIAZUDDIN, S., SMITH, R. J., AHMAD, W., MULLER, U., HAMMERSCHMIDT, M., FRIEDMAN, T. B., LEAL, S. M., AHMAD, J. and KUBISCH, C. (2011). Loss-of-function mutations of ILDR1 cause autosomal-recessive hearing impairment DFNB42. *Am J Hum Genet* 88: 127-137.

CHEN, J. N. and FISHMAN, M. C. (1996). Zebrafish tinman homolog demarcates the heart field and initiates myocardial differentiation. *Development* 122: 3809-3816.

CHENG, J., ZHU, Y., HE, S., LU, Y., CHEN, J., HAN, B., PETRILLO, M., WRZESZCZYNSKI, K. O., YANG, S., DAI, P., ZHAI, S., HAN, D., ZHANG, M. Q., LI, W., LIU, X., LI, H., CHEN, Z. Y. and YUAN, H. (2011). Functional mutation of SMAC/DIABLO, encoding a mitochondrial proapoptotic protein, causes human progressive hearing loss DFNA64. *Am J Hum Genet* 89: 56-66.

COLANTONIO, J. R., VERMOT, J., WU, D., LANGENBACHER, A. D., FRASER, S., CHEN, J. N. and HILL, K. L. (2009). The dynein regulatory complex is required for ciliary motility and otolith biogenesis in the inner ear. *Nature* 457: 205-209.

DROR, A. A. and AVRAHAM, K. B. (2010). Hearing impairment: a panoply of genes and functions. *Neuron* 68: 293-308.

EISEN, J. S. and SMITH, J. C. (2008). Controlling morpholino experiments: don't stop making antisense. *Development* 135: 1735-1743.

EKKER, S. C. and LARSON, J. D. (2001). Morphant technology in model developmental systems. *Genesis* 30: 89-93.

FRIEDMAN, T. B. and GRIFFITH, A. J. (2003). Human nonsyndromic sensorineural deafness. *Annu Rev Genomics Hum Genet* 4: 341-402.

FROLENKOV, G. I., BELYANTSEVA, I. A., FRIEDMAN, T. B. and GRIFFITH, A. J. (2004). Genetic insights into the morphogenesis of inner ear hair cells. *Nat Rev Genet* 5: 489-498.

GERETY, S. S. and WILKINSON, D. G. (2011). Morpholino artifacts provide pitfalls and reveal a novel role for pro-apoptotic genes in hindbrain boundary development. *Dev Biol* 350: 279-289.

GHYSEN, A. (2003). The origin and evolution of the nervous system. *Int J Dev Biol* 47: 555-562.

GILLESPIE, P. G. and MULLER, U. (2009). Mechanotransduction by hair cells: models, molecules, and mechanisms. *Cell* 139: 33-44.

GLEASON, M. R., NAGIEL, A., JAMET, S., VOLOGODSKAIA, M., LOPEZ-SCHIER, H. and HUDSPETH, A. J. (2009). The transmembrane inner ear (Tmie) protein is essential for normal hearing and balance in the zebrafish. *Proc Natl Acad Sci USA* 106: 21347-21352.

HADDON, C. and LEWIS, J. (1996). Early ear development in the embryo of the zebrafish, Danio rerio. *J Comp Neurol* 365: 113-128.

HAN, Y., MU, Y., LI, X., XU, P., TONG, J., LIU, Z., MA, T., ZENG, G., YANG, S., DU,

J. and MENG, A. (2011). Grhl2 deficiency impairs otic development and hearing ability in a zebrafish model of the progressive dominant hearing loss DFNA28. *Hum Mol Genet* 20: 3213-3226.

HE, Y., YU, H., SUN, S., WANG, Y., LIU, I., CHEN, Z. and LI, H. (2013). Trans-2-phenylcyclopropylamine regulates zebrafish lateral line neuromast development mediated by depression of LSD1 activity. *Int J Dev Biol* 57: 365-373.

HILGERT, N., SMITH, R. J. and VAN CAMP, G. (2009). Forty-six genes causing nonsyndromic hearing impairment: which ones should be analyzed in DNA diagnostics? *Mutat Res* 681: 189-196.

KARLSSON, J., VON HOFSTEN, J. and OLSSON, P. E. (2001). Generating transparent zebrafish: a refined method to improve detection of gene expression during embryonic development. *Mar Biotechnol (NY)* 3: 522-527.

KELLEY, M. W. (2007). Cellular commitment and differentiation in the organ of Corti. *Int J Dev Biol* 51: 571-583.

KIM, H. Y. and GLADYSHEV, V. N. (2004). Methionine sulfoxide reduction in mammals: characterization of methionine-R-sulfoxide reductases. *Mol Biol Cell* 15: 1055-1064.

KIMMEL, C. B., BALLARD, W. W., KIMMEL, S. R., ULLMANN, B. and SCHILLING, T. F. (1995). Stages of embryonic development of the zebrafish. *Dev Dyn* 203: 253-310.

KWON, T. J., CHO, H. J., KIM, U. K., LEE, E., OH, S. K., BOK, J., BAE, Y. C., YI, J. K., LEE, J. W., RYOO, Z. Y., LEE, S. H., LEE, K. Y. and KIM, H. Y. (2014). Methionine sulfoxide reductase B3 deficiency causes hearing loss due to stereocilia degeneration and apoptotic cell death in cochlear hair cells. *Hum Mol Genet* 23: 1591-1601.

LE GUELLEC, D., MORVAN-DUBOIS, G. and SIRE, J. Y. (2004). Skin development in bony fish with particular emphasis on collagen deposition in the dermis of the zebrafish (Danio rerio). *Int J Dev Biol* 48: 217-231.

LEE, B. C., DIKIY, A., KIM, H. Y. and GLADYSHEV, V. N. (2009). Functions and evolution of selenoprotein methionine sulfoxide reductases. *Biochim Biophys Acta* 1790: 1471-1477.

LEGER, S. and BRAND, M. (2002). Fgf8 and Fgf3 are required for zebrafish ear placode induction, maintenance and inner ear patterning. *Mech Dev* 119: 91-108.

MA, E. Y., RUBEL, E. W. and RAIBLE, D. W. (2008). Notch signaling regulates the extent of hair cell regeneration in the zebrafish lateral line. *J Neurosci* 28: 2261-2273.

NAGIEL, A., ANDOR-ARDO, D. and HUDSPETH, A. J. (2008). Specificity of afferent synapses onto plane-polarized hair cells in the posterior lateral line of the zebrafish. *J Neurosci* 28: 8442-8453.

NAYAK, G. D., RATNAYAKA, H. S., GOODYEAR, R. J. and RICHARDSON, G. P. (2007). Development of the hair bundle and mechanotransduction. *Int J Dev Biol* 51: 597-608.

ROBU, M. E., LARSON, J. D., NASEVICIUS, A., BEIRAGHI, S., BRENNER, C., FARBER, S. A. and EKKER, S. C. (2007). p53 activation by knockdown technologies. *PLoS Genet* 3: e78.

TIAN, T., ZHAO, L., ZHAO, X., ZHANG, M. and MENG, A. (2009). A zebrafish gene trap line expresses GFP recapturing expression pattern of foxj1b. *J Genet Genomics* 36: 581-589.

USAMI, S., ABE, S., SHINKAWA, H. and KIMBERLING, W. J. (1998). Sensorineural hearing loss caused by mitochondrial DNA mutations: special reference to the A1555G mutation. *J Commun Disord* 31: 423-434; quiz 434-425.

WATERMAN, R. E. and BELL, D. H. (1984). Epithelial fusion during early semicircular canal formation in the embryonic zebrafish, Brachydanio rerio. *Anat Rec* 210: 101-114.

WEISSBACH, H., ETIENNE, F., HOSHI, T., HEINEMANN, S. H., LOWTHER, W. T., MATTHEWS, B., ST JOHN, G., NATHAN, C. and BROT, N. (2002). Peptide methionine sulfoxide reductase: structure, mechanism of action, and biological function. *Arch Biochem Biophys* 397: 172-178.

WEISSBACH, H., RESNICK, L. and BROT, N. (2005). Methionine sulfoxide reductases: history and cellular role in protecting against oxidative damage. *Biochim Biophys Acta* 1703: 203-212.

WHITFIELD, T. T. (2002). Zebrafish as a model for hearing and deafness. *J Neurobiol* 53: 157-171.

WU, G. F., HOU, Y. L., HOU, W. R., SONG, Y. and ZHANG, T. (2010). Giant panda ribosomal protein S14: cDNA, genomic sequence cloning, sequence analysis, and overexpression. *Genet Mol Res* 9: 2004-2015.

XU, Q. (1999). Microinjection into zebrafish embryos. *Methods Mol Biol* 127: 125-132.

ZHAO, X., ZHAO, L., TIAN, T., ZHANG, Y., TONG, J., ZHENG, X. and MENG, A. (2010). Interruption of cenph causes mitotic failure and embryonic death, and its haploinsufficiency suppresses cancer in zebrafish. *J Biol Chem* 285: 27924-27934.

Web references

http://hereditaryhearingloss.org/main.aspx?c=.HHH&n=86307

http://www.gene-tools.com/Oligo_Design

http://zfin.org/zf_info/anatomy/dict/current.html

http://www.ensembl.org

http://www.ncbi.nlm.nih.gov/unigene?term=msrb3